

NEW DEVELOPMENT AT THE JINR HEAVY ION CYCLOTRON FACILITY

G.Gulbekyan, Yu.Oganessian, I.Kolesov, B.Gikal, A.Morduev,
 O.Borisov, A.Ivanenko, V.Kutner, V.Bekhterev
 Flerov Laboratory of Nuclear Reactions,
 Joint Institute for Nuclear Research,
 Dubna, Moscow reg., 141980, Russia

ABSTRACT

The Heavy Ion Cyclotron Facility of the Flerov Laboratory of Nuclear Reactions is designed for the acceleration of ions from H to U with the energies ranging from 20 up to 100 MeV/nucleon.^{?)} The facility consists of 2 compact cyclotrons i.e. U-400 and U-400M, the age of the first one is about 14 years. The U-400M cyclotron can be used as a post-accelerator or as the one with independent PIG or ECR ion sources. Its construction was started in 1989. In May 1991 we got the first internal beam of ⁴He¹ with the energy of 30 MeV/n and the intensity of 10¹⁴pps on the U-400M with the PIG ion source. At present we have got internal beams of light ions up to Ne and the energies up to 53 MeV/n. In 1992 we are going to realize the extraction system, the beam lines and the beam commissioning for the first experiment. We are planning to use the U-400 as an injector in 1993.

1. INTRODUCTION

The lay-out of the JINR U-400-U-400M Heavy Ion Cyclotron Facility is presented in Fig.1. Table 1 presents the characteristics of the U-400 injector-cyclotron operating since 1978. At present the cyclotron is used for the purposes of nuclear physics and applied researches, for the production of nuclear filters, for radiation study of materials. The cyclotron is equipped with 12 beam channels.

Every month we have about 20 changes of the type of ion used. The tuning time is 4 hrs. Annually the cyclotron is operated for about 5000 hrs.

At present the beam is extracted by the charge exchange on the graphite foil with the charge exchange ratio $\frac{Z_2}{Z_1}$ from 2 to 5. In 1992 there will be realized the electrostatic extraction of a low-energy beam with the energy ranging from 0.5 to 2.8 MeV/n for the injection into the U-400M cyclotron. The line for the beam transportation from the U-400 to the U-400M is basically ready. Fig.2 presents the dependence of the U-400 beam intensity on the ion mass.

Table 1.

| | |
|------------------------|-----------------------------------------------------------------|
| Magnet weight | 2100 t |
| K-factor | 625 |
| Pole diameter | 4 m |
| Gap in the valley | 30 cm |
| Gap on the hill | 7 cm |
| Average magnetic field | 1.93÷2.14 T |
| Number of sectors | 4 |
| Spiral angle | 0 |
| Number of dees | 2 |
| RF range | 5.6÷12 MHz |
| RF harmonics | 2, 4, 6 |
| Voltage on the dees | 80÷100 kV |
| $\frac{Z}{A}$ range | 0.2÷0.028 |
| Ion energies | 22÷0.4 MeV/n |
| Source | PIG |
| Beam extraction | -via charge exchange(1978) -by electrostatic deflector(1992) |
| Vacuum | 7 x 10 ⁻⁷ torr |
| Power input | 1 MW |

The U-400M compact cyclotron is built basing on the magnet of the classical cyclotron of ions U-300 which worked at the laboratory from 1959 to 1989. The characteristics of the U-400M cyclotron are presented in Table 2.

Fig.3 presents a scheme of the U-400 beam injection into the U-400M cyclotron. The movable stripping foil is installed on the equilibrium radius.

The internal beam parameters of the U-400M + PIG are presented in Table 3.

The goal for 1992 is to obtain maximum intensities on the extracted beams of ²²Ne⁶⁺ and ¹⁸O⁵⁺ for the purposes of the first experiments.

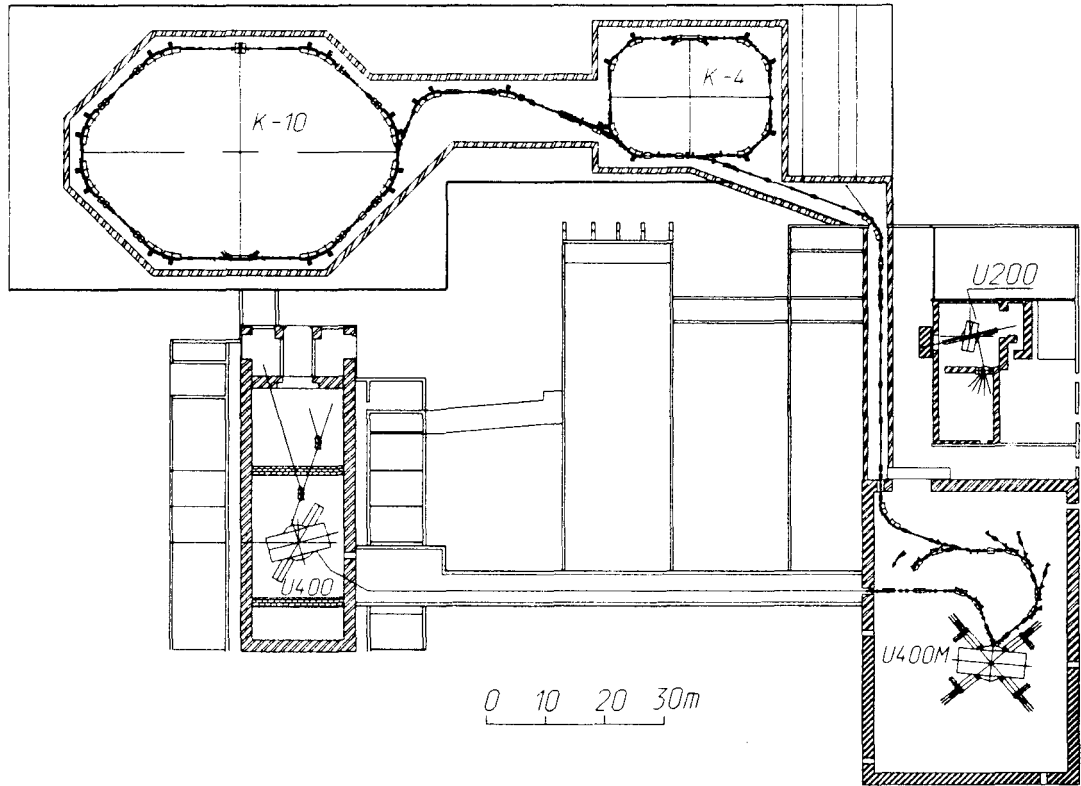


Fig.1. The lay-out of the cyclotron complex

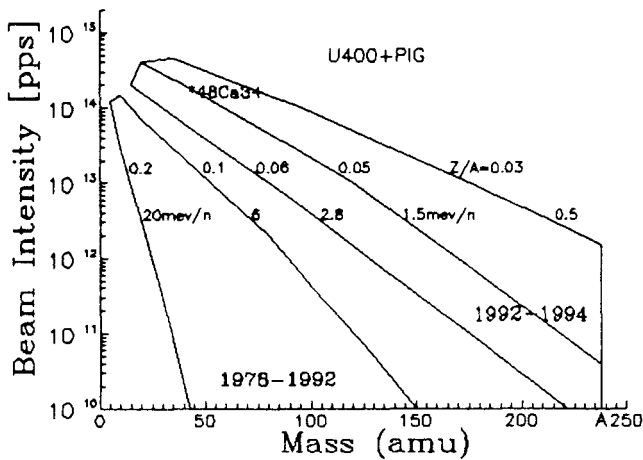


Fig.2. The dependence of the U-400 external beam intensities on the ion masses and energies.

Table 2.

| | |
|------------------------|-------------------------------------------------------------|
| Magnet weight | 2300 t |
| Pole diameter | 4 m |
| Gap in the valley | 50 cm |
| Gap on the hill | 10 cm |
| Average magnetic field | 1.5÷1.93 T |
| Number of sectors | 4 |
| Spiral angle | 40° |
| Number of dees | 4 |
| Frequency range | 11.5÷24.5 MHz |
| RF harmonics | 2, 3, 4, |
| Voltage on the dees | 130÷200 kV |
| $\frac{Z}{A}$ range | 0.5÷0.1 |
| Ion energies | 100÷6 MeV/n |
| Source | PIG (1991) ECR (1994) |
| Beam extraction | -via charge exchange(1992) -by magnetic deflectors(1992) |
| Power input | 1 MW |

2. MAGNETIC FIELD OF THE U-400M CYCLOTRON

The magnetic core cross section was increased by 10% and the excitation of the magnet was increased to $1.16 \times 10^6 \text{ A}$. The isochronous shape of the average magnetic field is determined by the thickness of the sectors

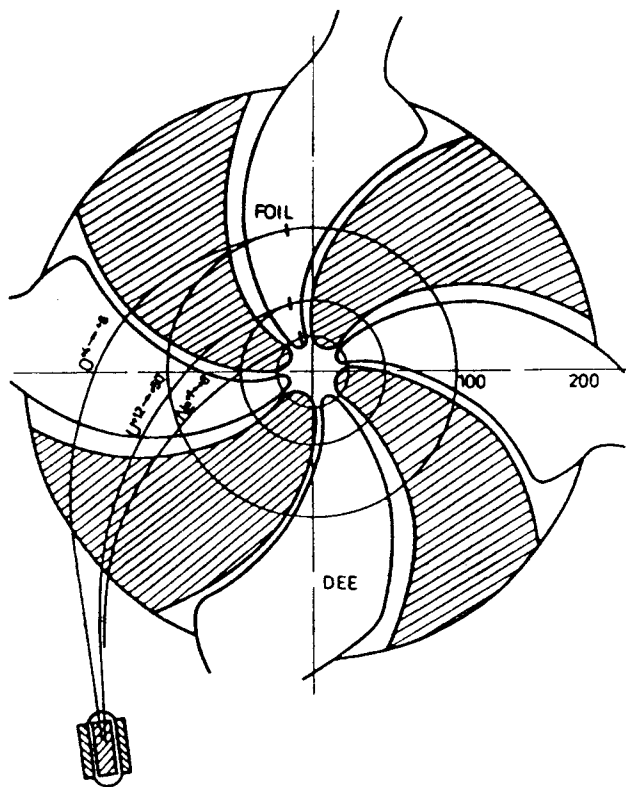


Fig. 3. The scheme of the injection into the U-400M.

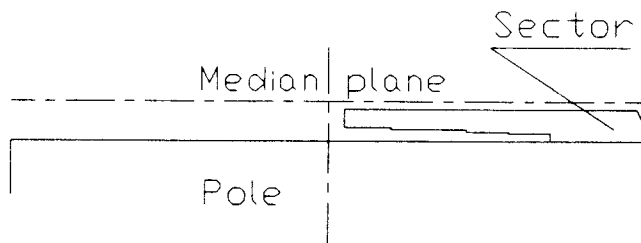


Fig. 4. The lay-out of the U-400M magnetic gaps with sectors.

which grows over the radius with the machining of the sector thickness performed from the pole side to decrease the influence of the machining depth step and to increase the flutter. (Fig.4). At the 1.5 T level of the average magnetic field in the center of the cyclotron the machining of the sector thicknesses ensures the isochronous radial growth of the magnetic field for ions with the energy of 100 MeV/n.

At the increase of the average magnetic field caused by the increase of the value of current in the main coil the radial growth of the magnetic field decreases at the rate of $0.26 \frac{T}{T}$. In this case the isochronous radial dependence of the average magnetic field is preserved with the accuracy of up to 0.01 T. Fig.5. Thus, the change of the magnetic field level in the cyclotron center from 1.5 T to 1.95 T ensures the isochronous acceleration of ions with $\frac{Z}{A}$ from 0.5 to 0.1 with the energy ranging from 100 to 6 MeV/nucleon with the minimum correction by the correcting coils (Fig.6).

In 1990 a full scale survey of the U-400M magnetic field was carried out. The measuring system moves in the polar coordinates. There are 14 InSb Hall probes on the block and 384 (0.9375) azimuthal and 8 (2 cm) radial steps for each Hall probe. We use usually as the radial coordinate the equilibrium orbit coordinate in the sector center, since the correcting shims and the trim coils are situated on the sector.

Fig.7 presents the flutter radial dependencies for ions with $\frac{Z}{A} = 0.5$ (100 MeV/n) and $\frac{Z}{A} = 0.2$ (22 MeV/n).

3. CORRECTING COILS

The U-400M correcting coils are used for the fine correction of the average magnetic field and of the radial gradients (10), for the correction of the median plane (3) and of the first harmonic(3). Hermetic blocks made of an aluminium alloy with 16 sector-type correcting coils are located on the surface of the sectors from the side of the median plane. The block has an autonomous vacuum pumping system. The block height is 28 mm. Multiturn coils are used. Each coil numbers from 20 to 30 turns. The cross section of the flat copper conductor is $6 \div 10 \text{ mm}^2$. The input current is reaching 30 A, i.e. the number of the ampere-turns in each coil is $400 \div 600$ at the current density of 3 A/mm^2 . The conductor has a min-

Table 3. Status for June 1992

| Ion | Energy(MeV/n) | Intensity(pps) |
|-----------------------|---------------|--------------------|
| $^4\text{He}^{1+}$ | 30 | 10^{14} |
| $^{12}\text{C}^{3+}$ | 30 | 2×10^{13} |
| $^{14}\text{N}^{3+}$ | 26 | 2×10^{13} |
| $^{14}\text{N}^{4+}$ | 40 | 2×10^{12} |
| $^{16}\text{O}^{3+}$ | 15 | 2×10^{13} |
| $^{16}\text{O}^{4+}$ | 30 | 3×10^{12} |
| $^{16}\text{O}^{5+}$ | 48 | 2×10^{12} |
| $^{20}\text{Ne}^{2+}$ | 6 | 5×10^{13} |
| $^{20}\text{Ne}^{4+}$ | 20 | 5×10^{12} |
| $^{20}\text{Ne}^{5+}$ | 30 | 3×10^{12} |
| $^{20}\text{Ne}^{6+}$ | 46 | 10^{12} |
| $^{40}\text{Ar}^{4+}$ | 6 | 2×10^{13} |
| $^{40}\text{Ar}^{5+}$ | 10 | 10^{13} |

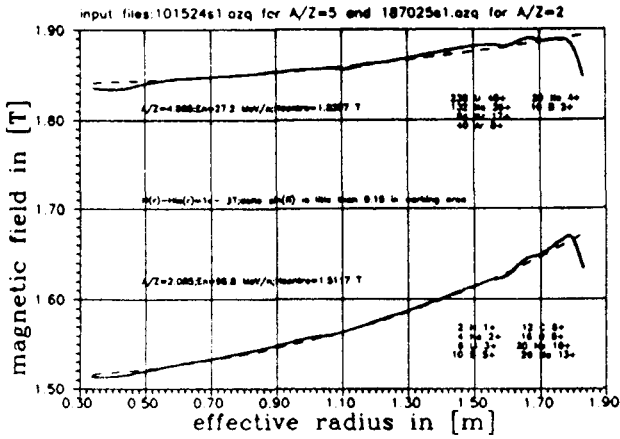


Fig. 5. Radial dependence of the effective magnetic field on level of the average magnetic field.

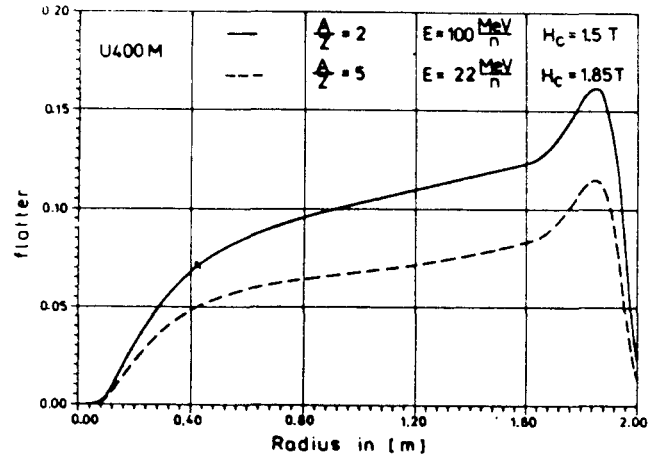


Fig. 7. The radial dependence of the flutter for $\frac{Z}{A} = 0.5$ (100 MeV/n) and $\frac{Z}{A} = 0.2$ (22 MeV/n).

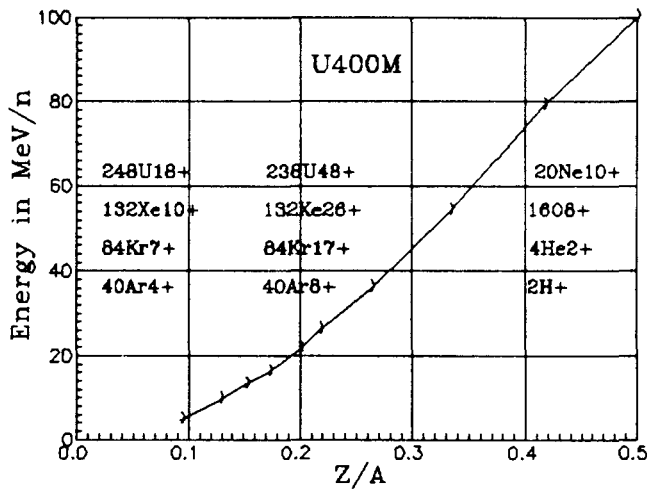


Fig. 6. The dependence of the U-400M ion energies on the $\frac{Z}{A}$ ratio.

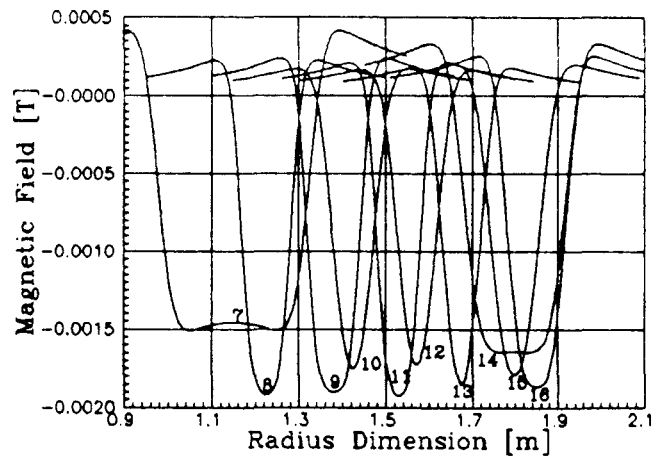


Fig. 8. The form-factor of 8 correcting coils at 100 ampere-turns in each.

eral and an epoxy insulation. The coils in each block are positioned consecutively over the radius one by one and in two layers. The upper layer is shifted versus the lower one to decrease the probability of dead zones apparition. The total dissipated power in the block is reaching 1 kW. The coils are glued and pressed to the internal surface of the aluminium blocks. All the coils of the same block use the same cooling circuit mounted over the block perimeter. The total power input of the correcting coils is 8 kW. The outputs are of a compact design. Fig. 8 presents the form-factor for 8 correcting coils.

Fig. 9 presents the effective magnetic field distinction from the isochronous one depending on the radius for ions with $\frac{Z}{A} = 0.5$ and of the energy of 100 MeV/n before and after the correction.

Fig. 10 demonstrates the radial dependence of the

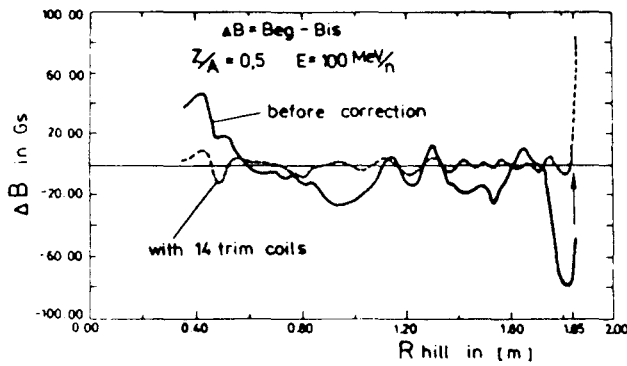


Fig.9. The distinction of the effective magnetic field from the isochronous one for ions with $\frac{Z}{A} = 0.5$ (100 MeV/n) before and after the correction.

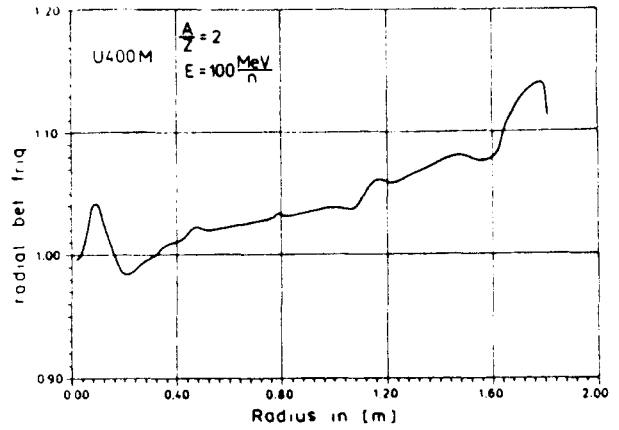


Fig.11. Radial dependence of the radial oscillations frequency for $\frac{Z}{A} = 0.5$ (100 MeV/n).

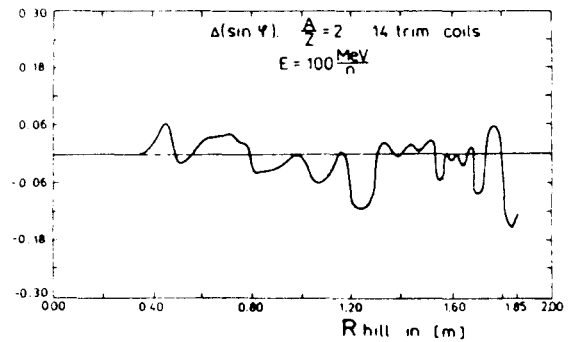


Fig.12. Phase motion of ions with $\frac{Z}{A} = 0.5$ and with the energy of 100 MeV/n.

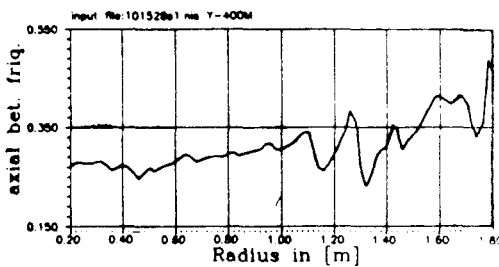


Fig.10. Radial dependence of the axial oscillations frequency for ions with $\frac{Z}{A} = 0.5$ (100 MeV/n).

axial oscillation frequency on the radius for the same ions and Fig.11 shows the radial dependencies of the radial oscillations frequency. Fig.12 presents the phase motion of these ions with the radius.

4. RF SYSTEM

The choice of a 4-dee system has been predetermined by the necessity to ensure the acceleration rate in the central region, the optimization of the phase motion through the increase of the orbits separation before the deflector. The U-400M acceleration system consists of 4 quarter-wave radial type coaxial resonators with the dee voltage of 200 kV. A dee with the angular length of 40° and the height of 100 mm is positioned in the valley and is installed in the machine by the radial movement of the resonance tank. The resonance tank of 1.34 m diameter and 3.5 m length and the stem of 0.68 m diameter form the induction part of the resonator with the wave impedance of 40 Ohm. Fig.13 presents a scheme of the U-400M resonator.

The dee has an aluminium frame. The reducing

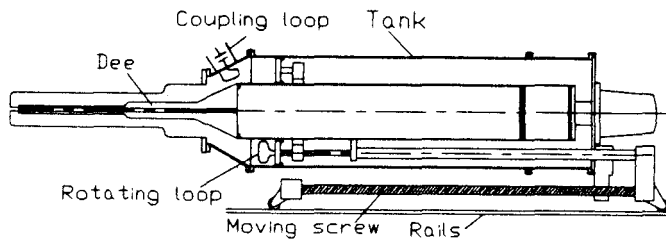


Fig.13. Lay-out of the U-400M resonator.

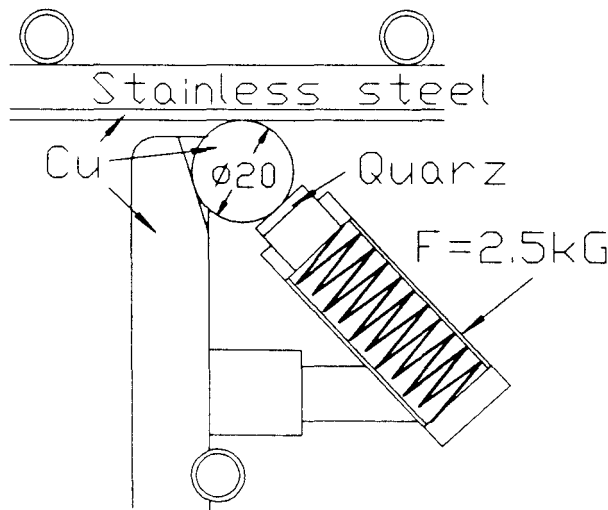


Fig.14. Scheme of the sliding contacts design.

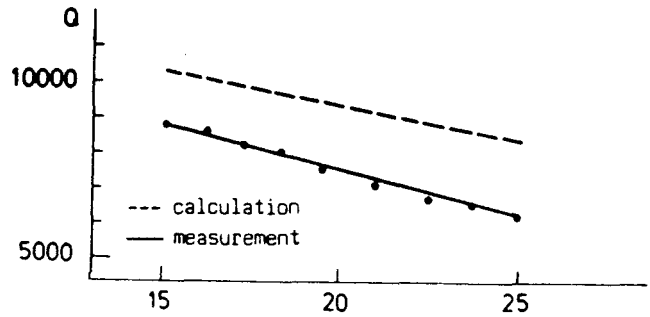


Fig.15. Dependence of the resonator quality on frequency.

pipe is made of copper-plated stainless steel by the explosion technology in Byelorussia. The resonance tank and the stem are made of copper-plated stainless steel by the diffusion technology with the subsequent machining in Russia. The cooling circuits are welded to the stainless steel from the outside at a step of $10 \div 20$ cm. Chromium-plated stainless steel rails are mounted inside the tank. A short-circuiting plate installed on a carriage moves by them. The accuracy of mounting is 0.1 mm which corresponds to the values ranging from 0.4 to 1 kHz. The short-circuiting plate is actuated by the rod through the back flange by means of a screw located under the tank outside. A short-circuited rotational fine-tuning loop with the area of 400 cm^2 is mounted on the short-circuiting plate and moves together with it. The loop ensures the $80 \div 120$ kHz range of fine frequency tuning. Sliding contacts are made of balls with the diameter of 20 mm and of hard oxy copper with a thermal quartz insulation and with the slapping force of 2.5 kg. The lay-out of the assembly operated for 1 year already on the U-400M with the current density up to 30 A/ball is presented in Fig.14.

This design is being operated on the CI-100 implanter for 4 years already with the current density of up to 300 A/ball. The reducing pipe homes a rotation connecting loop with the area of 300 cm^2 which is connected with the 60 Ohm feeder through a retunable compensation capacitor. Fig.15 presents the dependence of the resonator quality on frequency. Fig.16 presents the dependence of the voltage distribution over the dee radius for different frequencies.

For the case of radio frequencies at a voltage reaching 200 kV and for the second harmonic the effective accelerating voltage is only 750 kV per turn. Four RF generators with the power of 20 kW are situated in a separate room and provide the dees with the voltage of 140-100 kV in the frequency range of $11.5 \div 24.5$ MHz. The start-up of the machine was performed by these generators. In 1992 the power of the generators will be increased to 80 kW and the dee voltage — to 200 kV. The voltage phase free drift on the dees is about 20° per hour because of a low current density and big gaps. The electron system ensures the phase control with the accu-

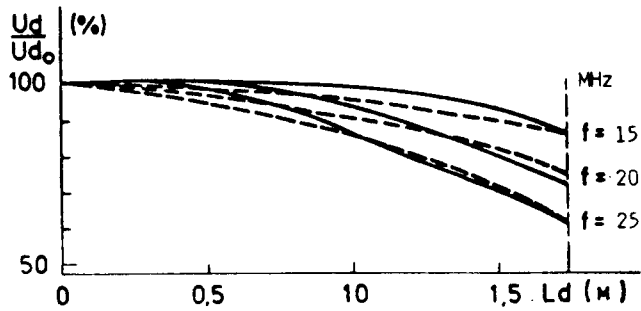


Fig.16. Radial distribution of the RF voltage of the U-400M cyclotron dee.

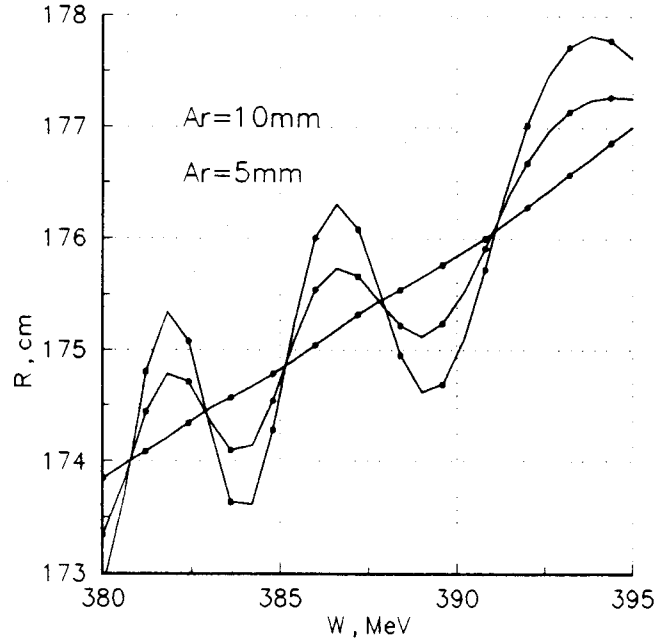


Fig.18. Radial oscillation of the beam with $\frac{z}{A} = 0.5$ around the equilibrium orbit and the effect of orbits separation growth.

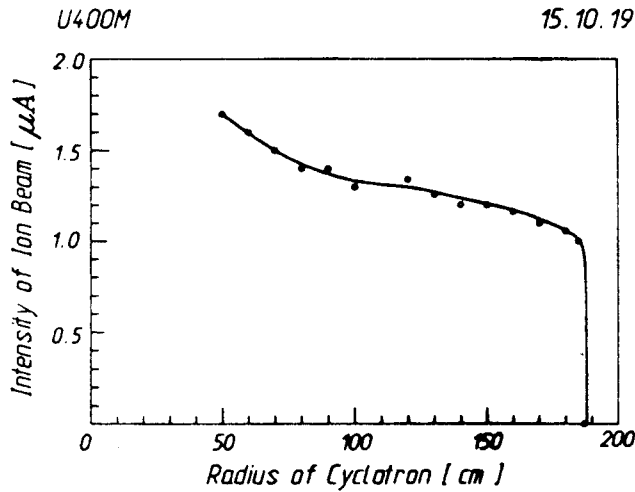


Fig.17. Radial distribution of the $^{12}\text{C}^{3+}$ beam intensity.

racy of 1° as well as the amplitude stabilization with the accuracy of 10^{-3} and is presently in the operating adjustment stage. The machine was started-up under strong multipactoring especially during the optimization of the feeder connection with the load caused by high quality, the presence of SiO_2 coming from the construction work and from the copper machining and by a low-level RF leak against the background of the generator start-up. At present the phenomenon of the resonance discharge is very seldom met.

5. THE U-400M VACUUM SYSTEM

The dismountable vacuum chamber of the U-400M consists of the cyclotron poles with octagonal aluminium alloy washers tightened around it. Racks are mounted at the corners of the polygon and the ladder-shaped seal for rectangular flanges and resonators are mounted along the perimeter. The pumping is performed by 6 diffusion pumps with LN_2 screens at the rate of 24000 l/sec. The volume of the vacuum chamber is 35 m^3 . The surface area is 375 m^2 . The pressure in the chamber 3×10^{-7} torr. The vacuum load is about 4×10^{-3} torr.l/sec. When a PIG-type internal source is used the process vacuum is 10^{-6} torr and the loss of the light ion beam is 50%. Fig.17 presents the radial distribution of the $^{12}\text{C}^{3+}$ beam intensity.

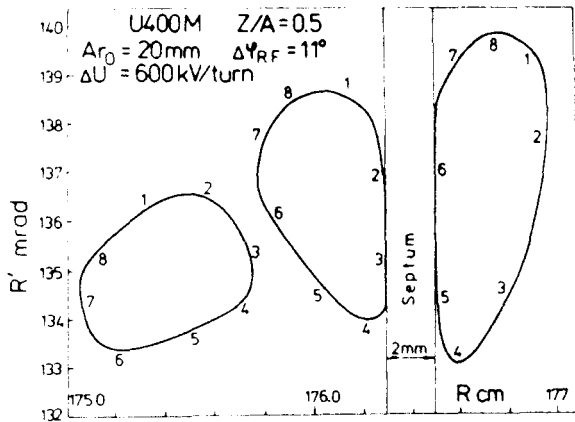


Fig.19. Transformation of the beam with $\frac{Z}{A} = 0.5$ phase portraits at the entrance into the sector during the last turns.

6. BEAM EXTRACTION SYSTEMS

The dees are installed in all the 4 valleys of the U-400M cyclotron. The gap in the sectors is 44 mm. Three electrostatic deflectors may be placed in the dees, but in this case the electric field intensity up to 140 kV/cm is to be used. On the other hand the energy separation of the orbits of the ions with $\frac{Z}{A} = 0.5$ (100 MeV/n) makes 2.7 mm at the radial oscillation frequency of $\nu_r = 1.15$. At the controlled amplitude and coherent oscillation phase the separation of orbits will be up to 10 mm. Fig.18 presents the radial oscillation of the beam with $\frac{Z}{A} = 0.5$ around the equilibrium orbit.

For ions with the energy of 22 MeV/n ($\frac{Z}{A} = 0.2$) just the energy separation of orbits will make 9 mm. Fig.19 presents the transformation of phase portraits at the sector entrance during the last turns of the beam with the energy of 100 MeV/n, RF phase width of 11° and the coherent oscillation amplitude of 20 mm. The beam emittance at the deflector entrance will be about 20 mm.mrad at the energy spread of 5×10^{-3} . The beam extraction will be carried out by 4 magnetic deflectors with the 2 mm thickness of the magnetic septum. The lay-out of the extraction system is presented in Fig.20.

Deflectors I and III are purely current ones without iron and the channels II and IV are of iron. The magnetic channels characteristics are presented in Table 4. The radial and axial envelope of the beam with the energy of 100 MeV/n ($\frac{Z}{A} = 0.5$) is shown in Fig.21.

The cross section of the first magnetic channel is presented in Fig.22.

The magnetic field distribution at the input current of 2500 A and the current density of up to 50 A/mm² are shown in Fig.23.

The second magnetic channel is placed into the dee and is equipped with the "wings" to compensate the dissipated field (Fig.24).

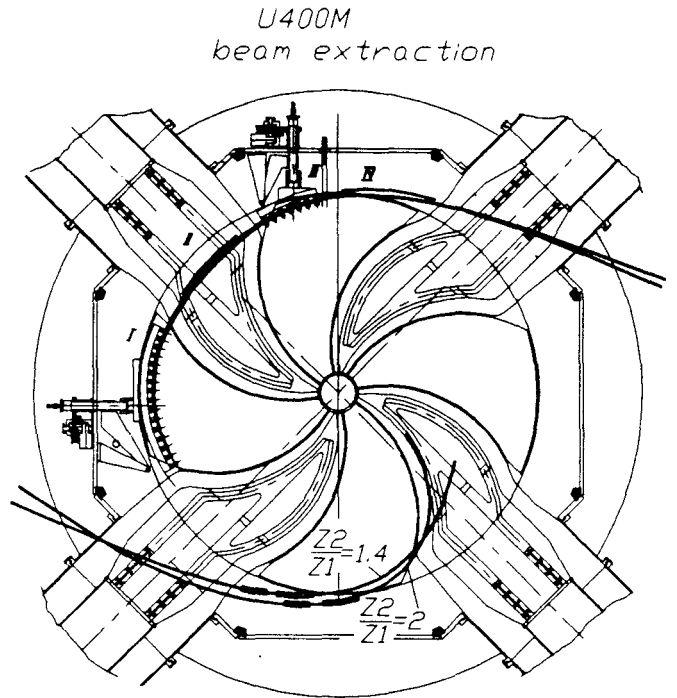


Fig.20. Lay-out of the U-400M beam outputs.

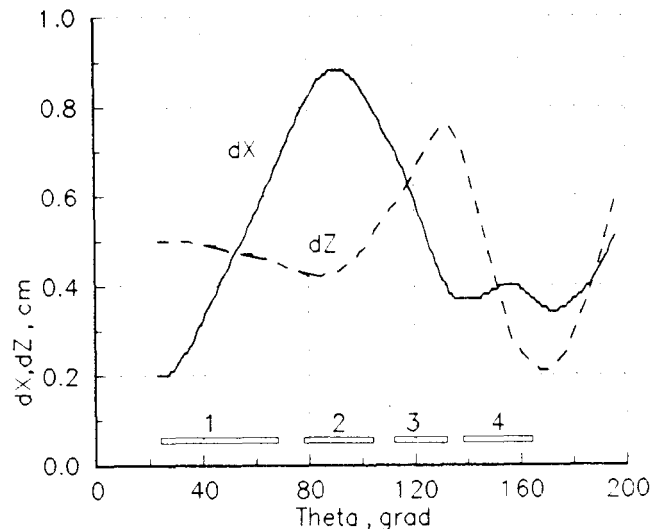


Fig.21. The radial and axial envelope of the beam.

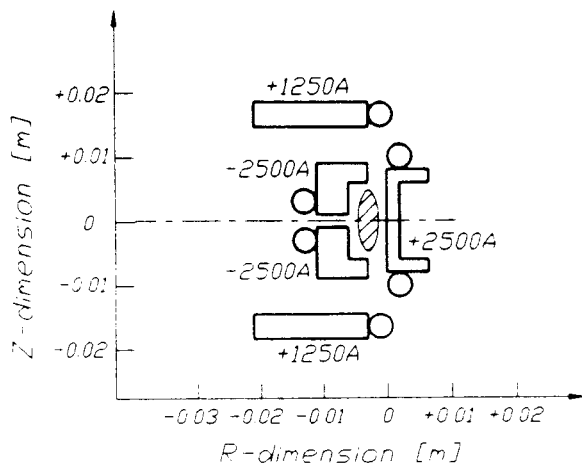


Fig. 22. Cross section of the first channel.

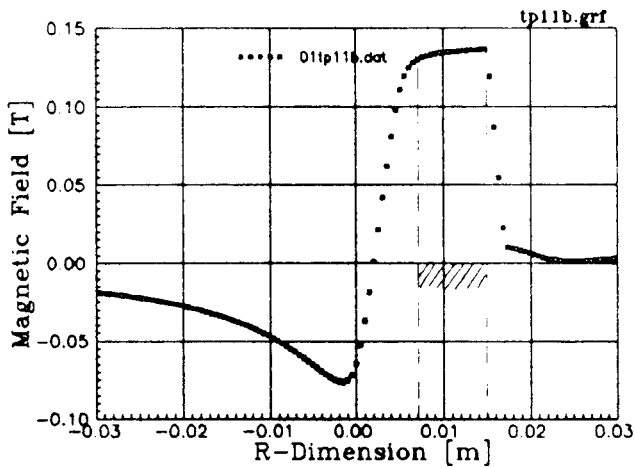


Fig. 23. Distribution of the first channel magnetic field.

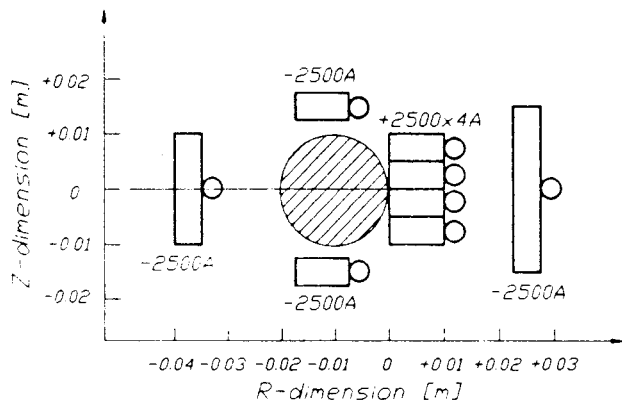


Fig. 24. Cross section of the 3-d channel.

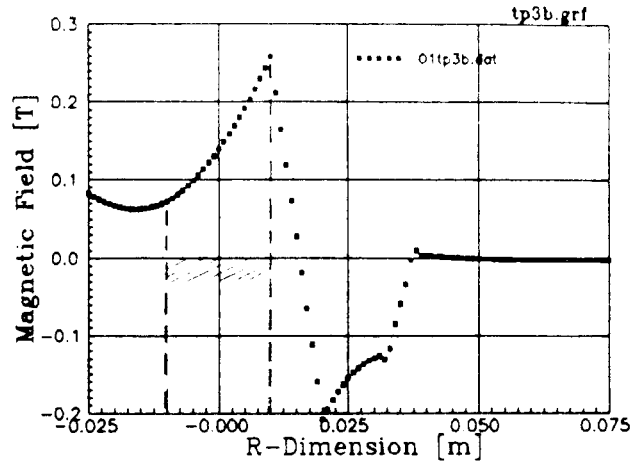


Fig. 25. Distribution of the 3-d channel magnetic field.

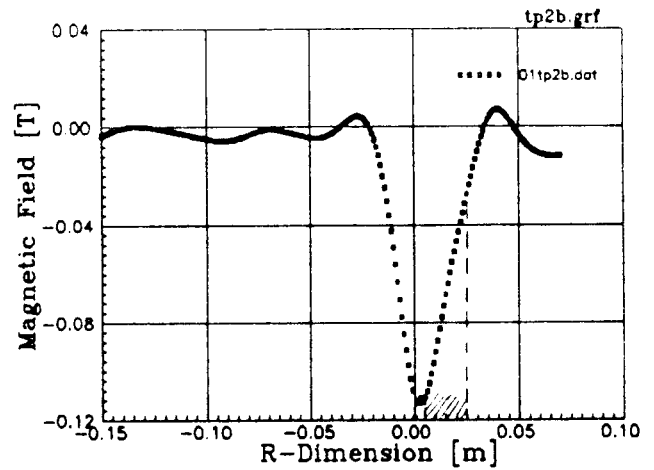


Fig. 26. Distribution of the 2-nd channel magnetic field.

The cross section of the 3-d magnetic channel (Fig. 25) and the magnetic field distribution are presented in Fig. 26.

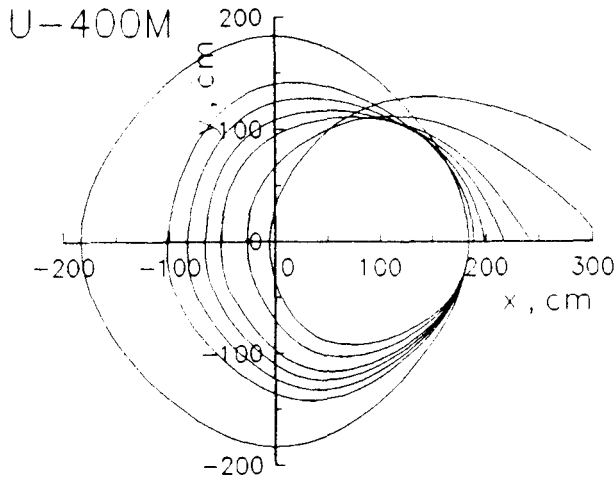
The beam extraction will be carried out in 1992.

7. BEAM EXTRACTION FROM THE U-400M BY THE CHARGE EXCHANGE

Beam extraction by the charge exchange on a thin graphite foil is the only one used on the FLNR U-200 and U-400 cyclotrons. This most convenient and flexible method allows to extract the beams with the RF phase range up to 40° without the emittance collimation by the deflectors apertures. The charge exchange ratio $\frac{Z_2}{Z_1}$ on the U-200 and U-400 cyclotrons is from 2 to 5. The radial beam drift based on the strong first harmonic of the magnetic field. The harmonic appears on the sector-valley boundary after the charge exchange is used. The separation of orbits is from 10 to 30 cm. On the U-400M cyclotron the characteristic range for the charge exchange ratio $\frac{Z_2}{Z_1}$ is from 1.1 to 2 and it appears impos-

Table 4.

| Channel No | ΔB (T) | | G (T/cm) | |
|------------|---------------------|---------------------|---------------------|---------------------|
| | $\frac{Z}{A} = 0.5$ | $\frac{Z}{A} = 0.2$ | $\frac{Z}{A} = 0.5$ | $\frac{Z}{A} = 0.2$ |
| 1 | -0.060 | -0.12 | 0 | 0 |
| 2 | -0.045 | -0.06 | 0.03 | 0.04 |
| 3 | -0.100 | -0.15 | 0.05 | 0.07 |
| 4 | 0.0 | 0.0 | 0.08 | 0.08 |



$Z_2/Z_1 = 1.3, 1.4, 1.5, 1.6, 1.8, 2.0$

Fig.27. Simulation of the motion of ions with the charge exchange ratios from 1.3 to 2 without changing the foil position.

sible to use the first harmonic of the magnetic field in the sector-valley region. The ion motion has been simulated. It is well seen from Fig.27 that there is a possibility of extracting the beam within the charge exchange ratio range of 1.3-2.

Ions in the range from 1.4 to 2 can leave freely the cyclotron vacuum chamber. The possibility of focussing the trajectories into one point at the transportation channel entrance due to the weak radial and azimuthal motion of the foil has been studied. Fig.28.

The calculated envelope function of the beam with the emittance of 10π mm-mrad when using two focussing channels is shown in Fig.29.

The beam extraction by the charge exchange will be used on the U-400M in the direction which is opposite to the deflectors output and will be used for the production of secondary beams of exotic nuclei on a thick target. The energies of ions extracted by the charge exchange are from 30 MeV/n ($^{12}\text{C}^3 \rightarrow ^{12}\text{C}^6$) to 60 MeV/n ($^{14}\text{N}^5 \rightarrow ^{14}\text{N}^7$). The dispersion over charges

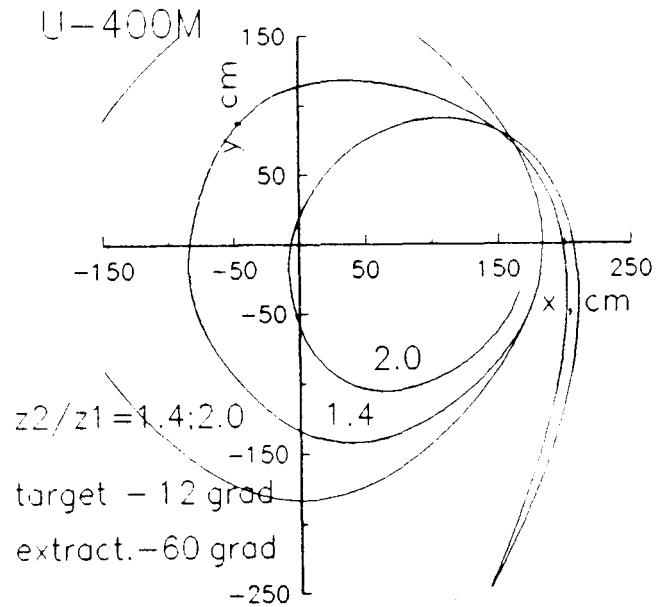


Fig.28. Focussing of the trajectories of ions with the charge exchange ratios from 1.4 to 2 onto the entrance into the transportation channel.

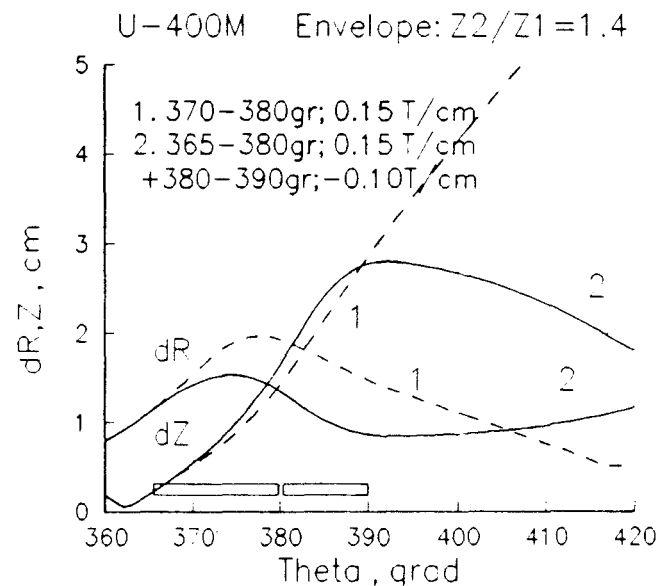


Fig.29. Beam envelope along the trajectory of extraction by charge exchange.

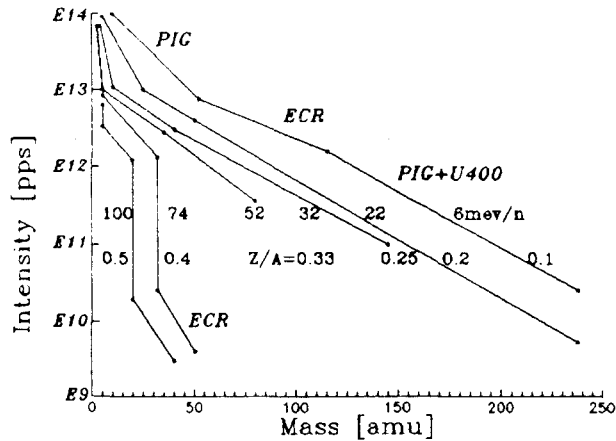


Fig.30. Intensities of the U-400+U-400M beams for different energies.

until medium mass ions (Ar, Ca, Fe, Ni) is insignificant. The life-time of foils is about 1 week at the beam intensity of 6×10^{12} pps. The beam extraction by the charge exchange will be performed in 1992.

The U-400M cyclotron can be used together with its own ion source as a post-accelerator after the U-400 and with independent PIG (1991) or ECR (1994) sources. The estimated beam intensities of the cyclotron complex for different energies are presented in Fig.30.

8. TRANSPORTATION CHANNELS

The lay-out of the U-400M cyclotron beams is presented in Fig.31. In 1992 it will be built of the elements manufactured in Romania, Russia and Estonia.

9. CONTROL SYSTEM

The control system is being developed on the basis of the CAMAC electronics and the IBM PC computers, connected into a local net. At present subsystems of control are built for the U-400M cyclotron itself.

10. CONCLUSION

The creation of the U-400M with a PIG-source will allow to start the experiments with fragmentation reactions and secondary beam generation reactions as early as in the beginning of 1993. Afterwards, new ion sources for the U-400M—U-400 and ECR will be eventually used. The U-400M is also the basic injector for the two-cooler project K4-K10 (Fig.1).

11. REFERENCES

- 1) Flerov, G.N. et al., Preprint 9-84-555, Dubna, 1984.

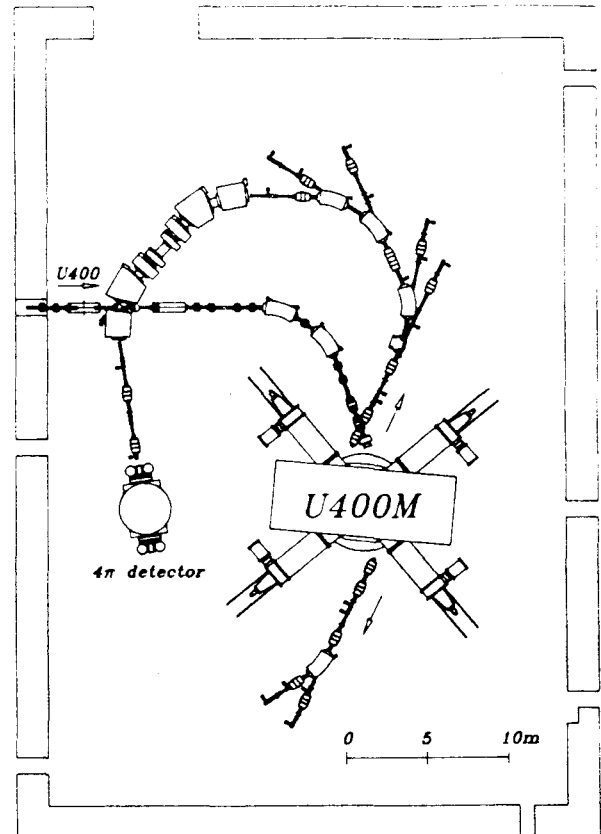


Fig.31. Lay-out of the U-400M beam channels.